RNase HI Depletion Strongly Potentiates Cell Killing by Rifampicin in Mycobacteria

Abeer Al-Zubaidi,[a,b] Chen-Yi Cheung,[c] Gregory M. Cook,[b,c] George Taiaroa,[d] Valerie Mizrahi,[e,f,g,h] J. Shaun Lott,[a,b] Stephanie S. Dawes[a,b]

[a]School of Biological Sciences, The University of Auckland, Auckland, New Zealand
[b]Maurice Wilkins Centre for Molecular Biodiscovery, The University of Auckland, Auckland, New Zealand
[c]Department of Microbiology and Immunology, School of Biomedical Sciences, University of Otago, Dunedin, New Zealand
[d]Department of Microbiology and Immunology, The Peter Doherty Institute for Infection and Immunity, The University of Melbourne, Melbourne, Victoria, Australia
[e]South African Medical Research Council, National Health Laboratory Service, University of Cape Town Molecular Mycobacteriology Research Unit, University of Cape Town, Cape Town, South Africa
[f]Department of Science and Technology/National Research Foundation Centre of Excellence for Biomedical TB Research, Institute of Infectious Disease and Molecular Medicine, University of Cape Town, Cape Town, South Africa
[g]Department of Pathology, University of Cape Town, Cape Town, South Africa
[h]Wellcome Centre for Infectious Diseases Research in Africa, University of Cape Town, Cape Town, South Africa

ABSTRACT Multidrug-resistant (MDR) tuberculosis (TB) is defined by the resistance of *Mycobacterium tuberculosis*, the causative organism, to the first-line antibiotics rifampicin and isoniazid. Mitigating or reversing resistance to these drugs offers a means of preserving and extending their use in TB treatment. R-loops are RNA/DNA hybrids that are formed in the genome during transcription, and they can be lethal to the cell if not resolved. RNase HI is an enzyme that removes R-loops, and this activity is essential in *M. tuberculosis*: knockouts of *rnhC*, the gene encoding RNase HI, are nonviable. This essentiality makes it a candidate target for the development of new antibiotics. In the model organism *Mycolicibacterium smegmatis*, RNase HI activity is provided by two enzymes, RnhA and RnhC. We show that the partial depletion of RNase HI activity in *M. smegmatis*, by knocking out either of the genes encoding RnhA or RnhC, led to the accumulation of R-loops. The sensitivity of the knockout strains to the antibiotics moxifloxacin, streptomycin, and rifampicin was increased, the latter by a striking near 100-fold. We also show that R-loop accumulation accompanies partial transcriptional inhibition, suggesting a mechanistic basis for the synergy between RNase HI depletion and rifampicin. A model of how transcriptional inhibition can potentiate R-loop accumulation is presented. Finally, we identified four small molecules that inhibit recombinant RnhC activity and that also potentiated rifampicin activity in whole-cell assays against *M. tuberculosis*, supporting an on-target mode of action and providing the first step in developing a new class of antimycobacterial drug.

KEYWORDS R-loop, RNase HI, antibiotic development, antibiotic resistance, antibiotic synergy, rifampicin

The emergence of drug-resistant bacteria has been recognized as a global health crisis (1). If left unchecked, antibiotic resistance threatens to overturn the substantial gains that have been made to human health care by the use of antibiotics to treat and prevent infectious disease, resulting in huge social and economic costs. Globally, the antibiotic resistance crisis has been spearheaded by the alarmingly rapid rise in the prevalence of *Mycobacterium tuberculosis* strains that are resistant to the cornerstone antibiotics of first-line tuberculosis (TB) therapy: rifampicin (which inhibits transcription) and isoniazid (which inhibits cell wall biosynthesis). The situation has been exacerbated
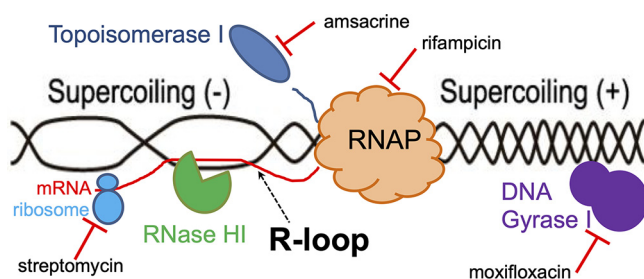
FIG 1 Twin domain model of transcription and location of enzymes (and their inhibitors) involved in topological modification or R-loop metabolism. RNAP, RNA polymerase I.

by the emergence and spread of extensively drug-resistant (XDR) *M. tuberculosis* strains that are also resistant to second-line TB therapeutics, such as the fluoroquinolones (which inhibit DNA topoisomerases) and linezolid (which inhibits the ribosome). It is estimated that there were at least 450,000 new cases of multidrug-resistant TB (MDR-TB) worldwide in 2019, and at least 180,000 deaths from MDR-TB were reported (2). The World Health Organization (WHO) has set a goal to eliminate TB by 2035, but this clearly cannot be achieved without addressing antibiotic resistance. Recently, striking progress has been made toward treating resistant disease, as in 2019, the U.S. Food and Drug Administration (FDA) approved a novel combination therapy that is able to treat both MDR- and XDR-TB disease effectively using three new antibiotics (bedaquiline, pretomanid, and linezolid), albeit with higher cost and greater side effects than standard first-line therapy (3). There have so far been no similar efforts toward improvements in first-line therapy, which is the primary line of defense, but clearly, retaining or improving the efficacy of the inexpensive first-line drugs for the treatment of drug-sensitive TB is imperative, as is enhancing their activity where possible to lower therapeutic doses and thereby reduce side effects and improve patient adherence.

Genome maintenance is essential for bacterial survival. Both transcription and replication processes inflict stresses that challenge genome topology and integrity. R-loops, which are RNA/DNA hybrids that form spontaneously in the genome during transcription, are a major threat to genome stability and can be lethal if not resolved (4, 5) (Fig. 1). Persistent R-loops can alter DNA topology, block both transcription and replication, and promote double-strand DNA breaks (DSBs) (6–9), although not all R-loops are pathological, since R-loop formation can be a necessary intermediate in plasmid replication (10) and in bacterial immune system surveillance via CRISPR (clustered regularly interspersed short palindromic repeats) (11). Multiple helicases and endonucleases contribute to the resolution of these hybrids, but RNase HI activity provides the major dedicated function for this, by targeted hydrolysis of the RNA strand in the RNA/DNA hybrid (12). Cells therefore require precisely controlled levels of RNase HI activity to prevent dysfunction. It was recently demonstrated that loss of RNase HI function in *Escherichia coli* drives the extinction of rifampicin- and streptomycin-resistant strains (13), suggesting that RNase HI might be a promising new antimicrobial target. RNase HI is already a validated target for HIV therapy, with the discovery and optimization of many specific and selective inhibitors of the RNase H activity of HIV-1 reverse transcriptase (14), some of which have promising antiviral activity coupled with low cellular toxicity (15, 16), although none as yet have been approved for clinical use.

The mycobacteria possess a bifunctional RNase HI enzyme called RnhC that is composed of an N-terminal domain with RNase HI activity and a C-terminal domain from the acid phosphatase family that possesses cobalamin-P phosphatase activity (CobC) and is involved in vitamin B_{12} biosynthesis (17–20). These domains can function separately, although the CobC domain confers increased activity on the RNase HI domain of *M. tuberculosis* RnhC (Rv2228c) via an unknown mechanism (17). Although most mycobacteria have only one gene encoding RNase HI activity, the nonpathogenic saprophytic model organism *Mycolicibacterium smegmatis* possesses a single-domain

RNase HI called RnhA in addition to RnhC. Both RNase HIs have been well characterized biochemically, as have single knockout strains of both *rnhA* and *rnhC* (18, 19, 21), which both grow indistinguishably from the wild type (18, 19). However, simultaneous deletion of both genes is lethal, reinforcing the essentiality of RNase HI activity in mycobacteria (18, 19). Transposon mutagenesis in *M. tuberculosis* located the essentiality of function to the RNase HI domain of RnhC (22, 23). Moreover, *M. tuberculosis rnhC* can rescue *M. smegmatis* from the lethality of the double knockout of *rnhA* and *rnhC* (20).

In this study, we used the dual RNase HIs of *M. smegmatis* to investigate RNase HI as a novel drug target in mycobacteria. We used single RNase HI knockout strains to deplete RNase HI activity and showed that deletion of RnhC in particular is sufficient to cause the accumulation of R-loops and to induce markers of genome topological stress. Furthermore, deletion of RnhC enhanced the killing activity of various antitubercular drugs, with an especially marked effect on rifampicin activity. We also identified four small molecules, previously shown to inhibit HIV RNase HI, as *in vitro* inhibitors of recombinant *M. tuberculosis* RnhC that also potentiate rifampicin killing in whole *M. tuberculosis* cells. Together, these results validate RNase HI as a drug target in the mycobacteria, demonstrate the potential for enhanced therapy by combining rifampicin treatment with RNase HI inhibitors, and open avenues to rescue rifampicin-resistant strains for therapy with rifampicin through RNase HI inhibition.

RESULTS

Loss of either *rnhA* or *rnhC* results in R-loop accumulation in *M. smegmatis*. To quantify R-loops in the RNase HI depletion strains, we isolated total nucleic acid from cultures of both Δ*rnhA* and Δ*rnhC* strains grown to mid-log phase and quantified the relative amounts of R-loops in each, using Southwestern blots with a monoclonal antibody specific for RNA/DNA hybrids (24). The specificity of the antibody for RNA/DNA hybrids was confirmed by subjecting samples to RNase HI digestion prior to detection and noting the loss of signal in control spots (Fig. 2A). R-loops were detected at a low level in the parental strain and accumulated in the Δ*rnhA* mutant by a factor of ~2-fold and in the Δ*rnhC* mutant by a factor of ~11-fold (Fig. 2B). This indicated that both RnhA and RnhC act as part of a protective system to remove R-loops in replicating and actively transcribing cells. In both cases, the accumulation of R-loops also indicated that neither the remaining RNase HI isoform, nor other potential hybrid removal mechanisms such as the DNA helicase RecG (25), are able to compensate fully for the loss of either RNase HI enzyme.

To confirm that loss of RNase HI activity was responsible for the observed increased abundance of R-loops in the Δ*rnhA* and Δ*rnhC* strains, we tested whether either *rnhA* or *M. tuberculosis rnhC* provided in *trans* could complement the Δ*rnhA* and the Δ*rnhC* mutants, respectively (Fig. 2). As expected, complementation with the plasmid-borne *rnhA* gene reduced the R-loop signal in Δ*rnhA* to a wild-type level (Fig. 2A). In contrast, introduction of a plasmid carrying *rnhC* into the Δ*rnhC* strain conferred a 3-fold increase of R-loops over Δ*rnhC* without plasmid. To determine whether the R-loop signal in the complemented strain might be plasmid-borne, we separated total nucleic acid on an agarose gel, transferred it to a nylon membrane, and carried out Southwestern blotting as before (Fig. 2C to E). Only the Δ*rnhC* strain showed the presence of R-loops, running as a smear of smaller fragments below the main band of chromosomal DNA. No R-loops were detected in the complemented strain, even after very long exposures (Fig. 2E), consistent with a reporter-based indication of restoration of normal topology by provision of *rnhC* in *trans* (see below). A dot blot with the same nucleic acid preparation used for the agarose gel electrophoresis (Fig. 2D) recapitulated the previous findings of excess R-loops in the Δ*rnhC* complemented strain, indicating that subjecting the sample to gel electrophoresis abolished the R-loop signal in the complemented strain but not in the Δ*rnhC* strain, showing that the R-loop signal observed in the dot blot of the complemented strain consisted of less stable or transient
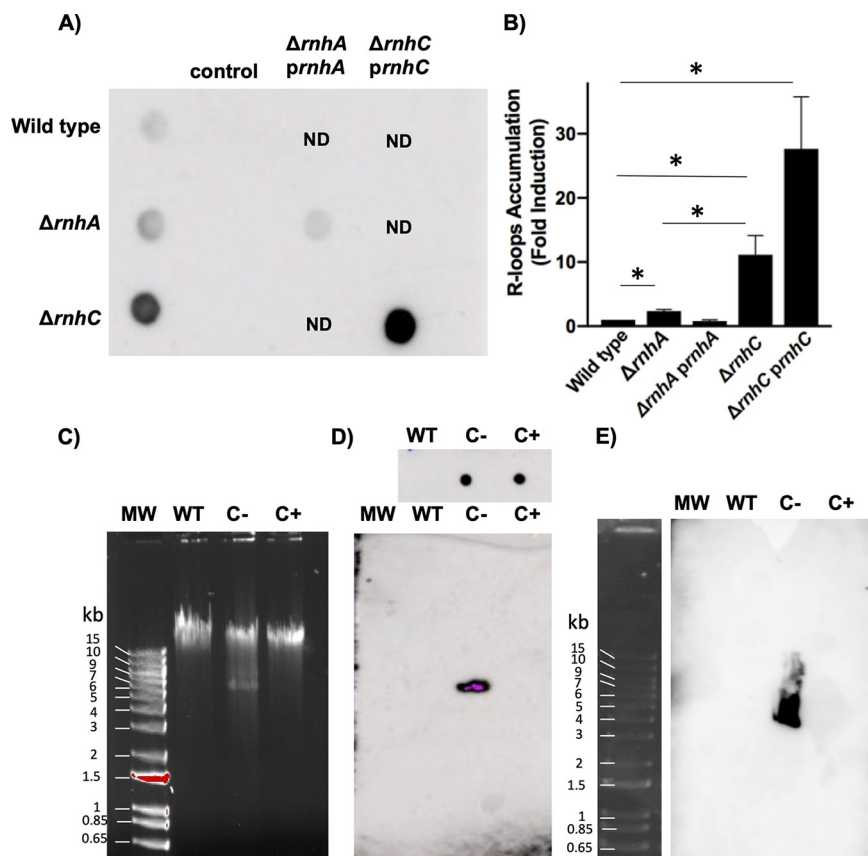
FIG 2 R-loop accumulation in wild-type, Δ*rnhA*, and Δ*rnhC* strains of *M. smegmatis* mc²155. (A) Dot-blot analysis of R-loop accumulation. Total nucleic acid from each strain was spotted onto the membrane and detected using the S9.6 RNA/DNA hybrid-specific monoclonal antibody. Control nucleic acid extracts were treated with *E. coli* RNase HI before spotting. (B) R-loops in the wild-type, Δ*rnhA*, and Δ*rnhC* strains, and their respective complemented strains were quantitated using Image Lab (Bio-Rad). Relative amounts are shown normalized to the wild type. (C) Uncut genomic DNA from the wild-type (WT), Δ*rnhC* (C−), or Δ*rnhC*-complemented strain (C+) was separated on a 1% agarose gel in duplicate. One set was stained with ethidium bromide as a record, and the other was transferred to a nylon membrane. (D) Genomic DNA from panel C (bottom panel) or applied as a dot blot (top panel) was probed with S9.6 monoclonal antibody to detect RNA/DNA hybrids. The bottom image was flipped horizontally to conform to the lane positions in panel C. (E) Extended exposure of an experimental repeat, showing smear of fragmented RNA: DNA hybrids migrating more quickly than bulk chromosomal DNA. The data shown are representative of the average of three independent experiments, with standard deviations indicated by error bars. The statistical significance of the differences was assessed using Student's unpaired *t* test calculated using GraphPad Prism 7. *, $P < 0.05$.

R-loops. R-loops that form in suboptimal regions of DNA under conditions of high topological stress, such as in small circular molecules undergoing active transcription, dissociate readily when topological stress is removed (26). Notably, the RNA/DNA hybrid signal corresponded to low molecular weight nucleic acid migrating below the bulk of the chromosomal DNA, indicating that the hybrid molecules were more sensitive to breakage than nonhybridized DNA, in keeping with their proposed role in generating double-stranded breaks. No low-molecular-weight nucleic acid was visible in the complemented strain, supporting the nonpathological nature of any R-loops captured in the cognate dot blot of the complemented strain. This conclusion is also congruent with subsequent experiments which showed full complementation with the complementation plasmid.

Loss of RnhC induces markers of DNA topology stress in *M. smegmatis*. Persistent R-loops, but not transient R-loops, could be expected to affect topology homeostasis. In light of the previous results, and since RnhC appeared to be the dominant contributor to R-loop resolution in *M. smegmatis*, we decided to probe topology homeostasis in the Δ*rnhC* mutant. In transcriptionally active cells, negative supercoils accumulate in
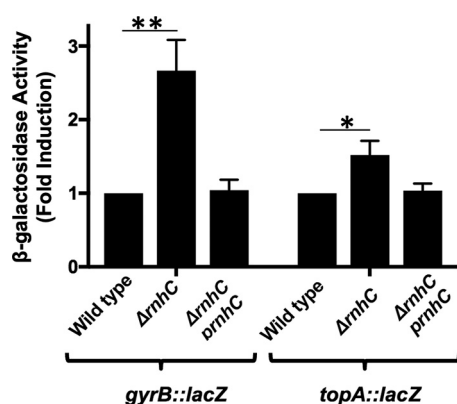
FIG 3 Expression of gyrase (*gyrB*) and topoisomerase I (*topA*) promoters fused to *lacZ* in wild-type, Δ*rnhC*, and complemented strains of *M. smegmatis* mc²155. The relative activities of the β-galactosidase reporters are shown, normalized to the wild type. The data shown are representative of the average of three independent experiments, with standard deviations indicated by error bars. The statistical significance of the differences was assessed using Student's unpaired *t* test calculated using GraphPad Prism 7. *, *P* = 0.02; **, *P* = 0.002.

the wake of the RNA polymerase, and positive supercoils accumulate ahead of it, a phenomenon known as the "twin domain hypothesis" (27, 28) (Fig. 1), which requires the activities of both topoisomerase I and DNA gyrase I to resolve (29, 30). Positive supercoils accumulate, in particular, between convergently oriented transcription units and also between converging replication complexes and transcription complexes, with negative supercoils accumulating upstream. Since negative supercoiling in the wake of the polymerases can promote R-loop formation, trapping the RNA polymerase on the DNA and providing a barrier to supercoil diffusion, we expected that there might be an increased demand in the Δ*rnhC* mutant for either topoisomerase I (which resolves negative supercoiling) or DNA gyrase I (which resolves positive supercoiling), or both, due to reduced ability to remove these R-loop barriers. Both the DNA gyrase and topo-isomerase I promoters in *M. smegmatis* are coupled directly to topological stresses experienced by the chromosome (responding by increasing expression up to 4-fold and 2-fold, respectively), as RNA polymerase binding elements (-35 and -10 sites) in each promoter adopt optimal conformations for transcription only if the DNA is either overwound (DNA gyrase) (31) or underwound (topoisomerase I) (32). An increase in expression of both promoters would therefore indicate an increased demand consist-ent with the presence of persistent R-loops (i.e., twin domains of positive and negative supercoiling generated by transcription but unable to be resolved by diffusion). We fused these promoters to a *lacZ* reporter gene and integrated these reporter cassettes into the *attB* site of the chromosomes of both wild-type and Δ*rnhC M. smegmatis* strains. Reporter activity from gyrase and topoisomerase promoters was increased significantly in the Δ*rnhC* strain compared to the wild type, by 3-fold (*P* = 0.002) and 1.7-fold (*P* = 0.02), respectively (Fig. 3). Notably, these increases in activity were abol-ished in the complemented Δ*rnhC* strain, suggesting first, that the Δ*rnhC* strain was experiencing increased levels of both positive and negative supercoiling and, second, that this topological stress was effectively relieved by the complementing *rnhC* gene provided in *trans*.

Loss of *rnhA* or *rnhC* increases plasmid copy number. Aberrant supercoiling sta-tus can affect control of plasmid replication mechanisms, which in turn can alter plas-mid copy number (10, 33–35). Notably, the pAL5000 origin of replication has been shown to be sensitive to phasing alterations which can either increase or decrease copy number (36). Read number comparisons from whole-genome sequencing (WGS) have been used to establish relative gene dosage (37), so we extended this concept to infer plasmid copy numbers relative to the chromosome. We carried out WGS of strains grown to mid-log phase to determine copy numbers of the pAL5000-based

TABLE 1 Determination of plasmid copy numbers by comparative read counts using whole-genome sequencing

| Strain [plasmid]	No. of reads	Genome coverage (×)	Plasmid coverage (×)	Plasmid copy no.[a]
Wildtype [pOLYG]	6,132,210	120	440	3.7
ΔrnhA [pOLYG]	6,465,798	126	2,667	21.2
ΔrnhA [prnhA]	6,333,356	122	3,186	26.1
Wild type [pBBK]	6,491,264	128	1,662	13.0
ΔrnhC [pBBK]	7,400,992	144	4,045	28.1
ΔrnhC [prnhC]	6,629,492	127	4,068	32.0

[a]Copy number was inferred from the ratio of plasmid coverage to genome coverage.

complementing plasmids in the ΔrnhA or ΔrnhC deleted strains (Table 1). The HygR-encoding vector backbone (pOLYG) was present at a copy number of 3.7 per genome in the wild type, which is consistent with reported values of 3 to 5 per cell (38), indicating that this method was indeed suitable for determining plasmid copy number. In contrast to the low copy number of the HygR-encoding plasmid in wild-type cells, the copy number of the KmR-encoding plasmid (pBBK) was present in wild-type cells at around 13 copies per genome, 4-fold greater than in the HygR-encoding plasmid.

Inspection of the plasmid sequence revealed a 12-bp deletion in the N terminus of the *repB* gene in the KmR-encoding vector backbone (see Fig. S1 in the supplemental material), leading to the deletion of one set of three tetrapeptide repeats. RepB belongs to the sigma factor family of proteins and is essential for plasmid replication (39). The C-terminal part of RepB binds to sites flanking the origin of replication, while the N terminus of RepB interacts with the C terminus of the RepA primase/polymerase and aligns it to bind to a highly conserved AT-rich sequence important for replication initiation (39). In previous work, it was determined that as little as a 3-bp deletion in the C terminus of RepA was sufficient to raise the copy number of the pHIGH100 replicon by 8-fold (40), suggesting that copy number can be affected by either alterations in RepA affinity for RepB or by a change in the relative alignment of RepA to the initiation region. A phase change equivalent to one helical turn of DNA in this region (+10 bp) increased the copy number 2-fold (36). The 12- bp deletion observed in RepB might therefore be responsible for the higher basal copy number in wild-type cells via a similar route, but investigation of the precise mechanism was not pursued further in this study.

Plasmid copy number was increased ~6-fold over wild-type levels to 21 per genome in the ΔrnhA mutant. In the ΔrnhC strain, the relative copy number of this plasmid was raised 2-fold over the wild-type level, to 28 per genome. Both the ΔrnhA and ΔrnhC strains therefore showed an increase in plasmid copy number over wild-type levels, although the initial effect on copy number was greater in ΔrnhA than in ΔrnhC. This suggested an involvement of either topology or R-loop homeostasis in copy number control. However, complementation with plasmid-borne *rnhA* or *rnhC* did not reduce the plasmid copy number to wild-type levels; instead, the trend was to increase it slightly. WGS confirmed that the *rnh*-deleted strains were isogenic with their respective complemented strains, eliminating compensatory mutations in host genes as a potential contributor to this effect. However, plasmid supercoiling status can differ markedly from chromosomal supercoiling status since host factors can be titrated to the chromosome (34). The observation of high levels of transient R-loops in the ΔrnhC-complemented strain might indicate higher levels of negative supercoiling or R-loops in the complementing plasmids, resulting in the sustained elevation of the copy number; however an investigation of the molecular basis for these high copy numbers was not undertaken.

Regardless of the precise mechanism, since R-loop accumulation could be complemented in *trans* by these plasmids in both the ΔrnhA and ΔrnhC strains, and the chromosomal DNA topology homeostasis was fully restored in ΔrnhC, we concluded that
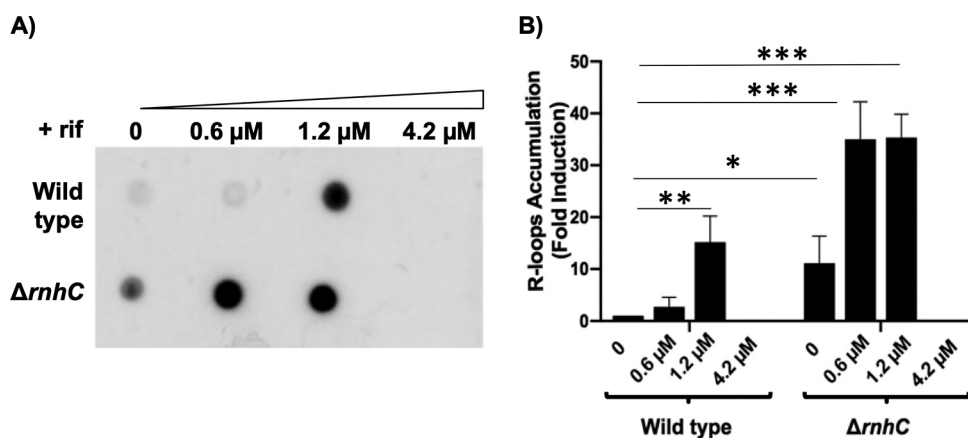
FIG 4 R-loop quantitation in wild-type and Δ*rnhC* strains of *M. smegmatis* mc^{2}155 after exposure to various concentrations of rifampicin. (A) Dot blot analysis of R-loop formation. (B) Quantification of R-loops observed in the dot blot, normalized to the wild-type strain in the absence of rifampicin. The data shown are representative of the average of three independent experiments, with standard deviations indicated by error bars. The statistical significance of the differences was assessed using Student's unpaired *t* test calculated using GraphPad Prism 7. *, $P < 0.05$; **, $P < 0.01$; ***, $P < 0.001$.

the plasmid copy number was well suited to the cellular requirements for RNase HI activity and that the increased copy number of the plasmid in the complemented strains might even reflect a useful cellular feedback mechanism to titrate the level of RNase HI appropriately. For these reasons, subsequent experiments were carried out using these constructs and strains.

Inhibition of transcription by low concentrations of rifampicin unexpectedly increases the accumulation of R-loops. Since transcription is a prerequisite for R-loop formation, we hypothesized that transcriptional inhibition would reduce the number of R-loops in the cell. Rifampicin, which binds to the RpoB subunit of RNA polymerase, inhibits transcription at the initiation step. Importantly, it does not affect RNA polymerase complexes that have added more than three ribonucleotides from proceeding to active transcription (41) and thus is not expected to uncouple transcription and translation in actively transcribing polymerases. Rifampicin has been used to reverse high levels of negative supercoiling in plasmids arising from transcription (42) and to reverse effects arising from R-loop accumulation (43, 44).

We exposed mid-log phase cultures of wild-type and Δ*rnhC* strains of *M. smegmatis* to rifampicin for 1 h before harvesting the cells and quantitating the R-loops present in them. Rifampicin at a concentration equivalent to the MIC$_{90}$ value for *M. smegmatis* (4.2 μM or 3.5 μg mL^{-1}) abolished R-loops, a result consistent with complete inhibition of transcription (Fig. 4). Surprisingly, both the wild-type and Δ*rnhC* strains contained significantly increased amounts of R-loops when exposed to a lower concentration of rifampicin (equivalent to the MIC$_{50}$ value; 1.2 μM or 1 μg mL^{-1}). A pronounced response to this low rifampicin exposure was shown by the Δ*rnhC* strain, with the number of R-loops increasing by approximately 3-fold compared to the nontreated Δ*rnhC* strain. Strikingly, even at a rifampicin concentration equivalent to the MIC$_{25}$ (0.6 μM or 0.5 μg mL^{-1}), more R-loops accumulated in Δ*rnhC* cells than in untreated cells, indicating an overload of the cellular systems required for R-loop resolution. This also suggested that the low number of R-loops observed in wild-type cells at this rifampicin concentration was not due to a lack of R-loop formation but, rather, was reflective of efficient resolution by RNase HI. Notably, R-loop resolution is clearly impaired even in wild-type cells exposed to rifampicin at the MIC$_{50}$. These results indicate that under these conditions, sublethal concentrations of rifampicin cause R-loop accumulation, a phenomenon that has not previously been described and is opposite to the effect of a lethal concentration of rifampicin.

Loss of RNase HI strongly sensitizes *M. smegmatis* to transcriptional inhibition. To better understand the cellular consequences of rifampicin-induced R-loop accumulation,
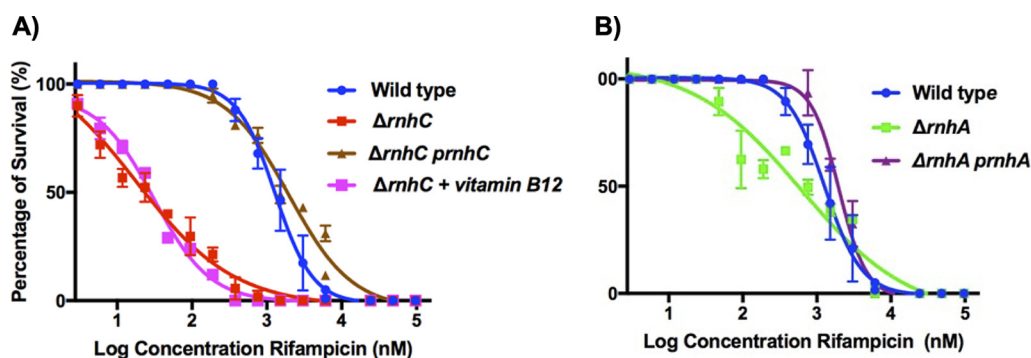
FIG 5 (A and B) Dose-response curves of rifampicin killing in (A) wild-type and $\Delta rnhC$ and (B) wild-type and $\Delta rnhA$ strains of *M. smegmatis* mc²155 and the respective complemented strains. The data shown are representative of the average of three independent experiments, with standard deviations indicated by error bars. When included, vitamin B_{12} was added to the growth medium at 10 μg mL^{-1}.

we carried out a dose-response assay to assess the extent to which RNase HI contributes to the survival of cells exposed to rifampicin. We found that wild-type *M. smegmatis* is inhibited as expected by previously established concentrations of rifampicin (45, 46). In contrast, loss of *rnhC* strongly sensitized the *rnhC* knockout strain to rifampicin, reducing the MIC$_{50}$ almost 100-fold, from 1.2 μM to 18 nM (Fig. 5A). This sensitivity was fully complemented by the provision of *rnhC* in *trans*. To confirm that this remarkable loss of viability under rifampicin stress is due to the loss of the RNase HI domain rather than the CobC domain of RnhC, which is involved in vitamin B_{12} biosynthesis (20), the assay was repeated in the presence of vitamin B_{12} in the growth medium. Supplementation with vitamin B_{12} altered the MIC$_{50}$ slightly, but not significantly ($P = 0.3$), from 18 nM to 30 nM (Fig. 5A), indicating that the rifampicin sensitization was due to the depletion of the RNase HI function of RnhC.

As the $\Delta rnhA$ strain of *M. smegmatis* showed a smaller accumulation of R-loops than the $\Delta rnhC$ strain (Fig. 2), we asked whether the loss of RnhA could also confer increased sensitivity to rifampicin. *M. smegmatis* $\Delta rnhA$ showed an approximately 3-fold increase in sensitivity to rifampicin compared to the wild type, which was fully complemented by the provision of *rnhA* in *trans* (Fig. 5B). Together, these findings indicated that depletion of RNase HI activity was responsible for the increased sensitivity of *M. smegmatis* to transcriptional inhibition and that loss of RnhA had a smaller contribution to this phenotype than the loss of RnhC. In fact, it was remarkable that such an apparently small contribution to R-loop metabolism still conferred synergy with rifampicin, underscoring the vulnerability of mycobacterial cells to even small amounts of RNase HI depletion.

Loss of RNase HI also sensitizes *M. smegmatis* to moxifloxacin and streptomycin. R-loop formation can be affected by uncoupling transcription and translation (47, 48) or by altering DNA supercoiling in the genome (5, 49). Rifampicin treatment does not uncouple transcription and translation, as it does not bind to polymerases that have added more than 3 ribonucleotides. Therefore, we tested the sensitivity of the *M. smegmatis* $\Delta rnhC$ strain to streptomycin (an inhibitor of translation), amsacrine (a topoisomerase I inhibitor), and moxifloxacin (a DNA gyrase inhibitor) (Fig. 1). As a control, we also investigated the sensitivity of the $\Delta rnhC$ strain to isoniazid, which disrupts mycobacterial cell wall synthesis by inhibiting mycolic acid synthesis (50).

The loss of the *rnhC* gene significantly reduced the MIC$_{50}$ for streptomycin, from 31 nM in the wild-type to 17 nM in the $\Delta rnhC$ strain ($P = 0.02$), and that for moxifloxacin, from 194 nM to 62 nM (Fig. 6A and B) ($P = 0.001$). In contrast, the loss of *rnhC* did not result in a significant increase in the sensitivity of *M. smegmatis* to amsacrine (MIC$_{50}$, 160 μM for the wild type and 140 μM for the $\Delta rnhC$ strain; $P = 0.8$) (Fig. 6C). As expected, the loss of the *rnhC* gene did not significantly affect the MIC$_{50}$ to isoniazid (101 μM for the wild type and 80 μM for the knockout strain, $P = 0.2$) (Fig. 6D).

Taken together, these results suggest that RNase HI inhibition would improve the efficacy of rifampicin, streptomycin, and moxifloxacin in a synergistic manner. In all cases, the increase in efficacy arising from RNase HI depletion was more pronounced
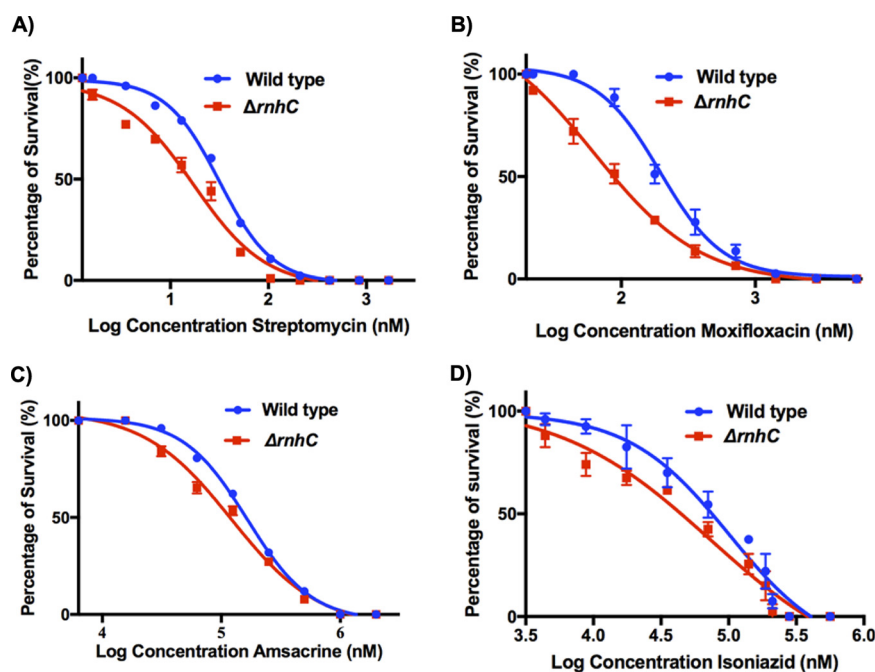
FIG 6 (A to D) Dose-response curves of antibiotic killing for (A) moxifloxacin, (B) streptomycin, (C) amsacrine, and (D) isoniazid in wild-type and Δ*rnhC* strains of *M. smegmatis* mc²155. The data shown are representative of the average of three independent experiments, with standard deviations indicated by error bars.

at sub-MICs of antibiotic, which is consistent with a requirement for some transcription to occur for the effect to be seen.

Drug candidates with diverse scaffolds inhibit recombinant *M. tuberculosis* RNase HI. The enhanced antibiotic activity observed when RNase HI activity is depleted in *M. smegmatis* indicated that RNase HI inhibition is likely to be compatible with existing antibiotics used for *M. tuberculosis* therapy. Effective RNase HI inhibitors would be of particular interest as synergistic partners for rifampicin, which is a key first-line antibiotic used to treat tuberculosis. Rifampicin is a powerful inducer of hepatic cytochrome P450 enzymes, which leads to antagonistic interactions with many other drugs (51). Hence, any drug that sensitizes *M. tuberculosis* to rifampicin also has the potential to improve therapeutic outcomes by decreasing the dose of rifampicin required.

Recently, specific inhibition of HIV RNase HI was reported (52–54), preventing viral replication in cells and supporting the possibility that small-molecule compounds could be similarly discovered for bacterial RNase HIs. The drug discovery effort against the RNase HI activity of HIV-1 reverse transcriptase has identified promiscuous chemical scaffolds that not only have activity on HIV RNase HI *in vitro*, but also have activity on *E. coli* RNase HI or human RNase HI. We therefore selected a small library of 33 inhibitors of the RNase H activity of HIV-1 reverse transcriptase (Table S4) which we screened for activity against recombinant *M. tuberculosis* RNase HI. Ten compounds were found to inhibit *M. tuberculosis* RNase HI at a concentration of less than 100 μM (Table S4).

Rifampicin synergy in whole-cell screens can eliminate off-target compounds. The 10 effective *in vitro* inhibitors of *M. tuberculosis* RNase HI were then tested for their antimicrobial activity against *M. tuberculosis* in a growth inhibition assay. All showed weak or no growth inhibition of *M. tuberculosis* when tested alone, which is consistent with their modest *in vitro* inhibition of RNase HI. Alternative explanations for this could be a lack of penetrance or off-target activity *in vivo*. However, we hypothesized that on-target inhibition of *M. tuberculosis* RNase HI *in vivo* would phenocopy the genetic depletion of RNase HI observed in *M. smegmatis* by increasing the sensitivity of *M. tuberculosis* to sub-MIC$_{50}$ concentrations of rifampicin. Four compounds (NSC353720, NSC600285, NSC18806, and NSC99726) significantly potentiated killing of *M.*
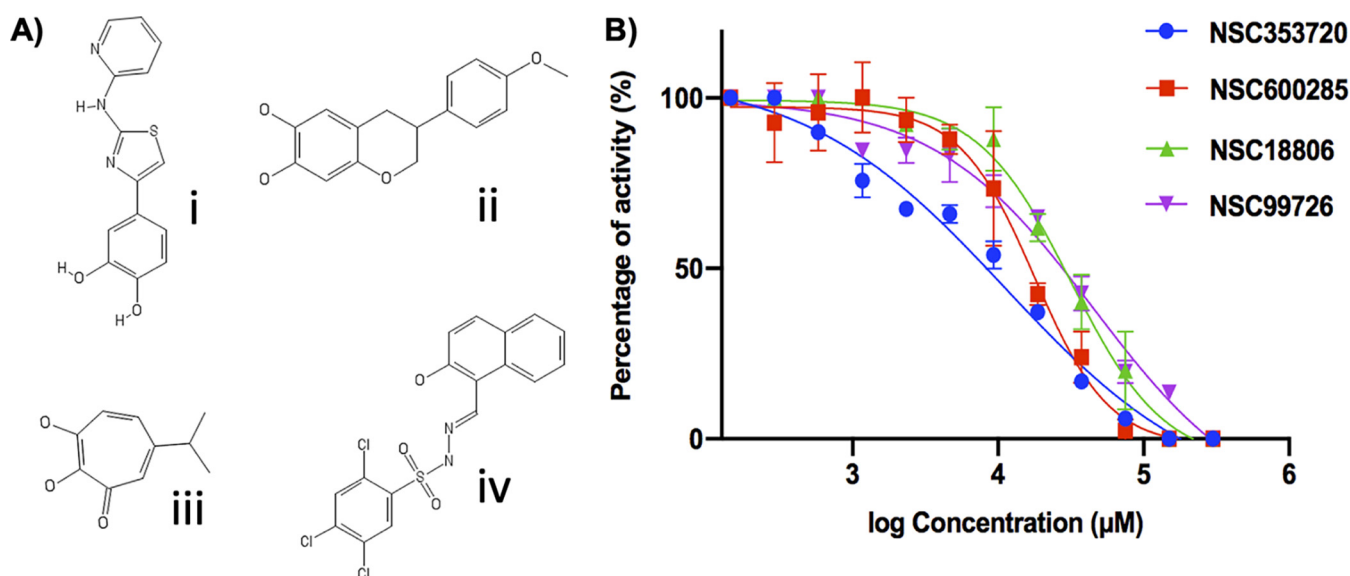
FIG 7 (A and B) Chemical structures (A) and dose-response curves (B) for NSC353720 (i), NSC600285 (ii), NSC18806 (iii), and NSC99726 (iv) against recombinant *M. tuberculosis* RNase HI. The data shown are the average of two independent experiments, with standard deviations indicated by error bars.

tuberculosis by rifampicin at a sub-MIC, indicating that they are likely to inhibit RNase HI *in vivo* (Fig. 7A and Table 2). *In vitro* dose-response curves against *M. tuberculosis* RNase HI show that NSC353720 (IC$_{50}$, 14 μM) was the most potent inhibitor, while NSC99726 was the weakest inhibitor (IC$_{50}$, 45 μM) of this compound set (Fig. 7B and Table 2).

DISCUSSION

R-loops are genotoxic stresses for all cells, and the resolution of these structures is critical for cell survival. RNase HI is the primary enzyme that resolves R-loops, although cells have evolved multiple mechanisms to reduce their occurrence or to repair them. In *M. tuberculosis*, RNase HI activity is essential for the growth of the bacterium *in vitro*, which makes it a potential drug target. Nevertheless, not much is known about the cellular consequences of RNase HI inhibition in the mycobacteria. In this study, we showed for the first time that depletion of RNase HI activity in *M. smegmatis*, by deletion of either of the two genes encoding RNase HI enzymes, caused an accumulation of R-loops. Loss of *rnhC* had a greater effect on R-loop accumulation than loss of *rnhA*.

The involvement of RnhC, and to a lesser extent RnhA, in the resolution of R-loops in *M. smegmatis* indicates that both enzymes are part of a protective system to remove the RNA/

TABLE 2 Inhibition of *M. tuberculosis* RNase HI recombinant protein and *M. tuberculosis* whole cells by RNase HI inhibitors and their interaction with rifampicin

Compound	*M. tuberculosis* RnhC IC$_{50}$ (μM)	*M. tuberculosis* MIC$_{90}$ (μM)		
		Compound alone	Compound + 5 nM rifampicin	FICI[a]
NSC353720	12	>512	64	0.3125
NSC353681	17	256	256	2
NSC600285	17	512	64	0.375
NSC600286	32	64	64	2
NSC143101	0.4	256	128	0.75
NSC18806	32	>512	128	0.5
NSC99726	45	512	64	0.375
NSC80693	11	256	256	1
NSC51535	2.8	>512	512	1
NSC117949	29	>512	512	1

[a]Interpretation of FICI: the cutoff for synergistic effect is ≤0.5, the cutoff for additive or indifferent effect is FICI >0.5 and <2, respectively, and the cutoff for antagonistic effect is FICI >2.
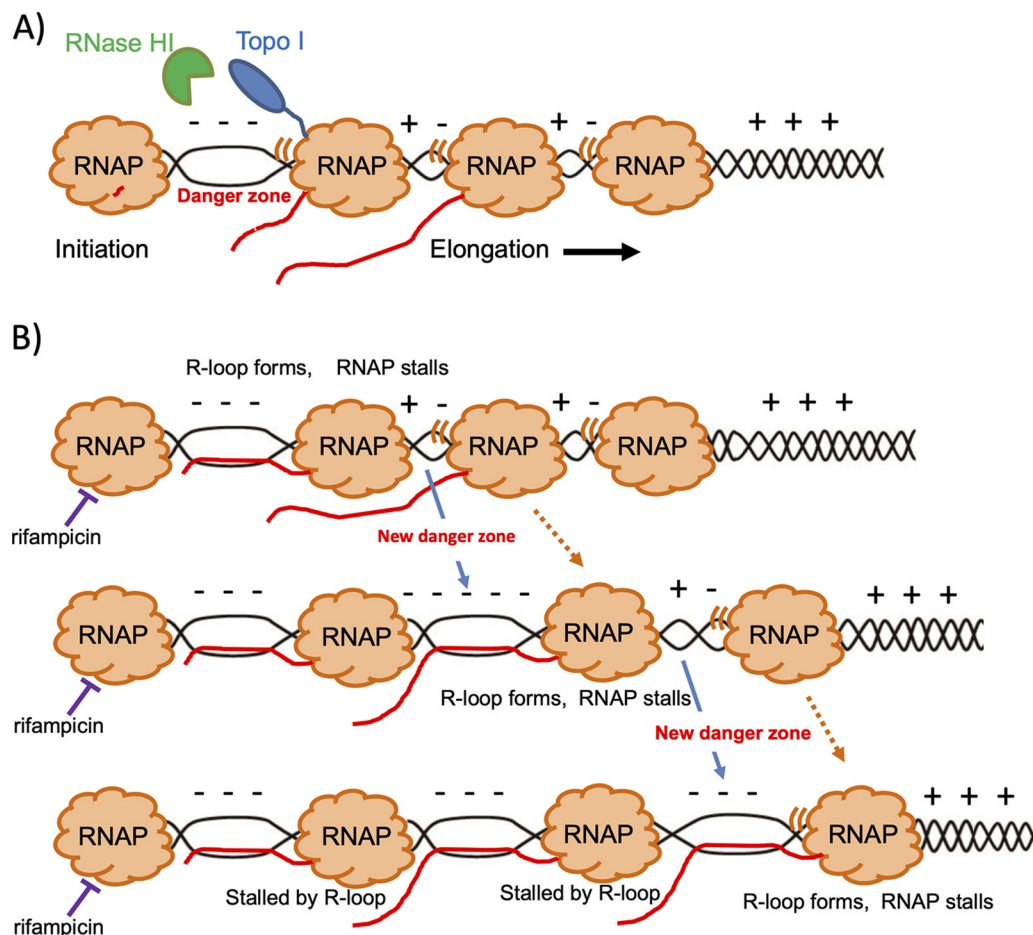
FIG 8 Domino effect model of R-loop formation under rifampicin stress. (A) Negatively supercoiled DNA (- - -) opens between a stationary RNAP (such as one in the promoter region) and a mobile RNAP (motion indicated by "((")). This danger zone for R-loop formation is policed by topoisomerase I (blue; shown only once for clarity), which competes with mRNA (red line; only shown twice for clarity) for underwound DNA and by RNase HI (green). Zones between mobile RNAP are more likely to be neutrally wound (+ -). (B) Under rifampicin stress, the promoter-bound RNAP cannot start elongating, the danger zone becomes critically underwound, and an R-loop forms and stalls its cognate RNAP. A new danger zone opens up between this stalled RNAP and its adjacent mobile RNAP. A new R-loop forms, stalling its RNAP, and the cycle continues until all mobile RNAP molecules are stalled by R-loops. Ribosomes are not shown.

DNA hybrids that form spontaneously in the genome during transcription before they induce DNA damage. The ability of *M. tuberculosis rnhC* to fully complement the Δ*rnhC* phenotype in *M. smegmatis* strongly suggests that RnhC carries out the equivalent role in both bacteria. Our data are consistent with previous reports showing that loss of RNase HI activity in *Bacillus subtilis* (55), *Saccharomyces cerevisiae* (56, 57), or human cells (58) resulted in the accumulation of R-loops.

Our striking finding that low levels of transcriptional inhibition promote R-loop accumulation (Fig. 4) gives new insight into R-loop metabolism. It is well established that polymerases which stall or backtrack during transcription are susceptible to forming R-loops (27, 28, 59–61) and that R-loop formation is able to stall translocating polymerases. The twin domain model of transcription shows that DNA in the wake of RNA polymerase becomes negatively supercoiled (i.e., underwound) and that DNA ahead of it becomes positively supercoiled (i.e., overwound) (30, 62, 63). For some promoters, transcriptional bursts result in loading of multiple RNA polymerase molecules (64) which tend to travel in convoys due to torsional constraints (65). Hence, in actively transcribed genes which contain polymerase convoys (66), the wake of unwound DNA from one polymerase is rewound by the following enzyme, thus reducing the need for topology-modifying enzymes, limiting backtracking (65, 67) and protecting this interpolymerase region of DNA from R-loop formation (Fig. 8A).

Thus, a topological balance exists in the DNA between actively transcribing RNA polymerases, which is disrupted if a polymerase is stalled.

Our results indicate that completely halting transcription with high levels of rifampicin abolishes R-loops, whereas lower levels of rifampicin increase R-loops through intermittent stalling of polymerases within the promoter region. This in turn severely affects cell viability in the absence of RNase HI. It is clear that an R-loop cannot arise directly from the rifampicin-bound polymerase, as no more than 3 nucleotides have been added to the transcript, so the R-loop must arise from an actively transcribing polymerase that is affected by this stalled polymerase in the promoter region. Stalled polymerases can provide barriers to supercoil diffusion. We hypothesize, therefore, that the last polymerase to have escaped the promoter will generate an increasing amount of underwound DNA, which promotes R-loop formation and which will likely stall this translocating polymerase. Further, if a convoy of polymerases is active in transcription, as occurs in instances of burst transcription, then a domino effect may be created over the length of the gene (Fig. 8B).

R-loop formation due to prevention of RNA polymerase escape from the promoter in this model requires at least one active polymerase that is affected by the stalled polymerase. Most R-loops are known to form in the 5′ end of genes, where cotranslational coupling may not yet have occurred. The most parsimonious explanation for this is that the affected polymerase is active on the same gene as the rifampicin-inhibited polymerase as shown in Fig. 8, but we cannot exclude longer-range effects on nearby active genes by similarly providing a barrier to supercoil diffusion. Divergently transcribed genes might be more susceptible in this case. Genes with high burst activity are more likely to have convoys of polymerases (64, 66), which might also be more prone to generating longer regions of negative supercoiling, and hence longer R-loops, as they are pulled along by the supercoiling forces generated by the leading polymerases in the convoy. Many *E. coli* genes have been shown to exhibit burst behavior dependent on the level of transcription (68, 69) or sigma factor recruitment (70). The proposed "domino effect" model of formation of R-loops under rifampicin stress is a thus a general, biologically plausible model based on previous models of polymerase activity (66, 71, 72) that nonetheless will be affected by the propensity of the DNA sequence to form R-loops, the availability of the nascent RNA to bind to DNA (i.e., whether transcription/translation is uncoupled), and potentially the "burstiness" of the promoter.

We showed that even partial loss of RNase HI activity through the deletion of *rnhC* or *rnhA* synergized extraordinarily well with transcriptional inhibition by rifampicin at concentrations below the MIC$_{90}$ (Fig. 5). This reveals an unappreciated role for RNase HI in promoting survival and possibly persistence under rifampicin stress. Rifampicin is one of the front-line drugs for TB therapy (2) and a vital component in resolving bacterial persistence *in vivo* (73). Notably, exposure to sub-MICs of rifampicin is thought to be instrumental in the emergence of antibiotic resistance in clinical settings. Our results suggest that inhibiting both RNase HI and transcription might act against the emergence of drug resistance, even in sub-MICs of inhibitors of both RNase HI and RNA polymerase. It also raises the possibility that RNase HI inhibition might rescue rifampicin as a treatment option in rifampicin-resistant bacteria, by increasing their sensitivity to its cellular effects.

Partial loss of RNase HI activity was compatible with isoniazid (Fig. 6D) and enhanced killing with moxifloxacin and streptomycin (Fig. 6A and B), indicating that in addition to providing a new target for drug development and enhancing first-line therapy, RNase HI inhibition would be a useful adjunct to second-line therapy as well. Uncoupling of transcription and translation is known to enhance R-loop production (48), and ribosomes can actively reverse stalled polymerases that might be more prone to R-loop formation (74). It is noteworthy, however, that the combination of translational inhibition and RNase HI depletion does not affect the cell as potently as the combination of transcriptional inhibition and RNase HI depletion. We speculate that in the context of actively translocating RNA polymerases, the opportunity for R-loop formation due to translational inhibition is

much reduced compared to the propensity for R-loop formation arising from stalled RNA polymerases, resulting in less synergy.

Many antibiotics, including rifampicin, are antagonistic with moxifloxacin (75), so the synergy of the latter with RNase HI depletion is both intriguing and valuable. We hypothesize that the synergy of moxifloxacin with RNase HI depletion might result from an increased number of gyrase/DNA complexes due to the 3-fold-increased expression of DNA gyrase (Fig. 1), resulting in a higher burden of double-strand DNA breaks (76).

Our finding that RNase HI depletion does not potentiate amsacrine lethality (Fig. 6C) contrasts with the synthetic lethal effect in *E. coli* of the loss of RNase HI and topoisomerase I (5). This apparent anomaly could be due to various factors. First, the expression of topoisomerase I is less effectively induced in the Δ*rnhC* strain than DNA gyrase I, which would be consistent with a topology-ameliorating effect of R-loops that has recently been proposed (26). Second, amsacrine is an uncompetitive inhibitor of topoisomerase I which binds to the topoisomerase I:DNA complex (77). Since topoisomerase I and mRNA are both localized by RNA polymerase and are both competing for the same under-wound DNA substrate, any R-loop formation would effectively remove underwound DNA as a substrate for topoisomerase I and proportionally reduce the binding of amsacrine to a DNA:topoisomerase I complex, an opposite effect to that seen with moxifloxacin. A final possibility is that, although amsacrine is on-target in eukaryotic cells and has been shown to inhibit *M. tuberculosis* topoisomerase I *in vitro* (77), it has not formally been shown that it does the same in mycobacterial cells. Topoisomerase I is an emerging drug target for development of anti-TB therapeutics. We predict that competitive inhibitors of topoisomerase I, which would more accurately mimic loss of the *topA* gene, might still be effective synergistic partners for RNase HI inhibitors.

R-loop formation is favored by high GC content and GC skew and is promoted by G4 quadruplex structures. Although sites susceptible to R-loop formation have not yet been mapped in the mycobacteria, over 10,000 sites for G4 quadruplexes in the *M. tuberculosis* genome have been predicted (78). The high (>65%) GC content of the mycobacterial genomes is likely to favor both the formation and the persistence of R-loops. If mycobacteria are more prone than other bacteria to R-loop formation due to their high GC content, this could account for the essential nature of RNase HI in the mycobacteria, since R-loops promote replication-transcription collisions (6, 7, 9, 55, 79), DNA recombination (6, 56, 80–82), DSBs (9, 82–84), and gene silencing.

The housekeeping nature of the enzymes involved in these synergistic combinations suggests that a wider application for combination therapeutics including RNase HI inhibitors also exists for other organisms. The loss of the *rnhC* gene in *Listeria monocytogenes* correlates with a loss of virulence in mice (55), and in *E. coli*, both streptomycin-resistant strains and rifampicin-resistant strains were competitively disadvantaged in Δ*rnhA* backgrounds (13). This indicates the potential for therapeutic aspects of RNase HI inhibition in bacteria even where RNase HI activity is not essential under laboratory conditions or where rifampicin tolerance is high.

This study identified four HIV RNase HI inhibitors that have activity against *M. tuberculosis* RNase HI *in vitro* and show synergy with rifampicin in a whole-cell assay (Fig. 6). The compound NSC600285 in particular is known to affect human RNase HI *in vitro* (https://pubchem.ncbi.nlm.nih.gov/bioassay/366) but is not toxic to eukaryotic cells unless the cells are deficient in DNA replication or repair, such as the Δ*rad50* and Δ*rad18* yeast strains (https://pubchem.ncbi.nlm.nih.gov/bioassay/155). This supports an on-target effect in eukaryotic cells and indicates that modifications are necessary to develop these chemical scaffolds for higher affinity and specificity for *M. tuberculosis* RNase HI. However, the inhibition we observe indicates that these scaffolds can penetrate both eukaryotic and prokaryotic cell walls, a key consideration for the delivery of antibiotics to intracellular pathogens such as *M. tuberculosis* and *L. monocytogenes*.

In combination, these lines of evidence strongly support an on-target effect on RNase HI *in vivo* for these compounds. However, the generation of resistant mutants to formally demonstrate on-target *in vivo* activity will require the development of compounds with

higher affinity. Crystal structures of the compounds in complex with *M. tuberculosis* RNase HI will allow more extensive structure-activity relationships to be established, and we are actively pursuing this approach. The use of rifampicin as a sensitizing compound will be advantageous in high-throughput screening, both for isolating compounds that might otherwise inhibit RNase HI too weakly to be identified in a normal growth inhibition screen and for prioritizing hits for further investigation and development.

In summary, this study validates RNase HI as a vulnerable, druggable target in the mycobacteria. It provides insight into R-loop metabolism in general and specifically highlights the contribution that low-level transcriptional inhibition makes to R-loop formation. It also demonstrates the proof of principle that this is a novel cellular susceptibility, which can be utilized as an antibacterial strategy. High-affinity inhibitors of RNase HI would be synergistic with some current first- and second-line antibiotics, with the potential to reduce the effective dose of rifampicin, with a concomitant reduction in side effects, and to reverse rifampicin resistance, rescuing this antibiotic for therapy.

MATERIALS AND METHODS

Strains, growth conditions, and media. The strains and plasmids used in this study are listed in Tables S1 and S2. *E. coli* strains Top10 and BL21(DE3)pLysS, used for cloning and protein expression, respectively, were grown in lysogeny broth (LB) and/or on agar at 37°C or 28°C in the presence of the appropriate antibiotic(s) at the following concentrations: 50 μg mL^{-1} kanamycin (GoldBio), 100 μg mL^{-1} ampicillin (GoldBio), 200 μg mL^{-1} hygromycin (Thermo Fisher), 5 μg mL^{-1} gentamicin (GoldBio) and 35 μg mL^{-1} chloramphenicol (Sigma-Aldrich). *M. smegmatis* mc^{2}155 and *M. tuberculosis* H37Rv were grown at 37°C in Middlebrook 7H9 broth (BD) or on Middlebrook 7H10 agar (BD) supplemented with 10% albumin-dextrose-saline, 0.2% glycerol, and 0.05% Tween 80 (Sigma) in the presence of appropriate antibiotics at the following concentrations: 25 μg mL^{-1} kanamycin, 50 μg mL^{-1} hygromycin, and 5 μg mL^{-1} gentamicin.

Plasmid and strain construction. Plasmids were constructed using standard cloning techniques. Inactivation of *rnh* alleles was carried out by homologous recombination with suicide plasmids (85) containing alleles inactivated by insertion of either a hygromycin antibiotic resistance cassette ($\Delta rnhC$) or kanamycin resistance cassette ($\Delta rnhA$). Allele replacement was confirmed initially by Southern blotting and subsequently by whole-genome sequence analysis (data deposited as BioProject no. PRJNA826235). Bioluminescent strains were constructed by transformation with the integrating plasmid pMV306G13+Lux, which carries the *luxABCDE* operon (86). *M. smegmatis rnhA* and *M. tuberculosis rnhC* genes for complementation studies were cloned into the pAL5000-based replicating plasmids (87) pOLYG (HygR) and pBBK (KmR), respectively, to make p*rnhA* (HygR) and p*rnhC* (KmR) (88). The *M. smegmatis rnhA* gene was cloned with 350 bp of the upstream region containing its own promoter (89), and in pBBK, *M. tuberculosis rnhC* was expressed from the well-characterized leaderless Ag85 promoter (90).

Statistical analysis. Drug dose-response curves were plotted, and 50% inhibitory concentration (IC$_{50}$) and MIC$_{50}$ determinations were carried out using nonlinear regression analysis. Student's unpaired t test was used to test for significance throughout. All plots and calculations were carried out using GraphPad Prism 7.

Immunodetection of RNA/DNA hybrids. Bacterial strains were grown as described above and harvested at mid-log phase (optical density at 600 nm (OD$_{600}$), 1.5). Nucleic acids were extracted from 20-mL culture aliquots using a modified phenol-chloroform technique (91): following lysozyme treatment, RNase A (10 μg/mL) was added to degrade single-stranded RNA, and small RNAs were precipitated by 30% (wt/vol) PEG 8000/30 mM MgCl$_2$. Nucleic acid was quantified using a spectrofluorometric method using QuantiFluor double-stranded DNA (dsDNA; Thermo Fisher). Nucleic acid (400 ng) was either separated by electrophoresis on a 1% agarose gel prior to transfer or was spotted directly onto Amersham Hybond N+ nylon membrane (GE Healthcare Lifesciences). The nucleic acid was air-dried and UV cross-linked to the membrane for 3 min using a transilluminator. Control aliquots were preincubated with 10 U of *E. coli* RNase HI (New England Biolabs [NEB]) for 2 h at 37°C before spotting. The membrane was blocked in TBST (20 mM Tris, pH 7.4, 150 mM NaCl, and 0.1% [vol/vol] Tween 20) containing 5% (wt/vol) milk powder at room temperature for 1 h, which was then removed and replaced with fresh TBST containing 5% (wt/vol) milk powder and S9.6 anti-DNA/RNA hybrid antibody (Kerafast) at 1 μg/mL and incubated at 4°C overnight. The following day, the membrane was washed (3 times for 5 min) with fresh TBST and finally incubated with a 1:1,000 dilution of horseradish peroxidase (HRP)-conjugated anti-mouse secondary antibody (Invitrogen) in TBST for 1 h at room temperature. Unbound secondary antibody was removed by washing (3 times for 5 min) with fresh TBST, and the blot was developed with West Pico PLUS chemiluminescent substrate (Thermo Fisher) according to the manufacturer's instructions. Chemiluminescence was detected using an Amersham Imager 600, and dot intensity was quantified using the Image Lab software suite (Bio-Rad).

β-Galactosidase reporter assay. Cultures of *M. smegmatis* mc^{2}155 and $\Delta rnhC$ were grown as described above and harvested at mid-log phase. Optical density was used for normalization of β-galactosidase activity. The assay was carried out according to Miller with variations (92, 93). Briefly, aliquots (2 mL) from each culture were harvested and resuspended in 600 μL of Z-buffer (60 mM Na$_2$HPO$_4$, 40 mM NaH$_2$PO$_4$, 10 mM KCl, 1 mM MgSO$_4$, 50 mM β-mercaptoethanol). Cells were permeabilized by adding 100 μL of chloroform and 50 μL of

0.1% SDS, and the mixture was incubated at 28°C for 5 min. Then 200 μL of ONPG (o-nitrophenyl-β-D-galacto-pyranoside; 4 mg/mL) was added to the mixture, which was incubated at 28°C until sufficient yellow color developed, and the time of incubation was recorded. The reaction was stopped by the addition of 500 μL of 1 M Na_2CO_3 and then the mixture was centrifuged at 10,000 $\times$ g for 2 min. The OD_{420} of the supernatant was measured, and the β-galactosidase activity was expressed in Miller units using the following equation: $OD_{420} \times 1,000/t \times v \times OD_{600}$, where t is the incubation time (min) and v is the volume of culture (mL).

Growth inhibition assays. (i) *M. smegmatis*. Two different methods were used to assess growth inhibition. (i) Agar proportion method: *M. smegmatis* strains were grown and harvested at mid-log phase (OD_{600}, 1 to 1.5). A single-cell suspension was prepared by centrifugation of the culture at 2,000 $\times$ g for 10 min to pellet clumps, the supernatant was collected, and 20% glycerol was added. Aliquots were snap-frozen in liquid nitrogen and stored at -80°C. For killing assays, 150 CFU were plated in Middlebrook 7H10 agar plates containing 2-fold serial dilutions of rifampicin and isoniazid and incubated at 37°C for 3 days. (ii) Bioluminescence reporter assay: bacterial strains carrying pMV306G13+Lux were grown as described above to mid-log phase (OD_{600}, 1.5) and diluted 30-fold to an OD_{600} of 0.05. All assays were set up in 96-well plates in a total volume of 100 μL, where 50 μL of the diluted culture was added to 50 μL of 2-fold serially diluted antibiotics in Middlebrook 7H9 medium. Two controls were added: bacteria only and medium only. The plates were sealed and incubated at 37°C for 18 h. Bioluminescence was quantified using a SpectraMax iD3 plate reader. Bacterial survival at each concentration was calculated based on the ratio of the relative light units (RLU) in the presence or absence of the inhibitor.

(ii) *M. tuberculosis*. *M. tuberculosis* mc^{2}6230 ($\Delta RD1$ $\Delta panCD$) (94) was grown in Middlebrook 7H9 broth supplemented with OADC (0.005% oleic acid, 0.5% bovine serum albumin, 0.2% dextrose, 0.085% catalase), 0.05% tyloxapol, and 25 μg mL^{-1} pantothenic acid (PAN) at 37°C. The assay was carried out in 96-well plates in a total volume of 100 μL. The cultures were diluted to an OD_{600} of 0.05, and 50 μL of the diluted culture was added to 50 μL of 2-fold serially diluted inhibitor in Middlebrook 7H9 medium. The plates were incubated without shaking at 37°C for 7 days before the MICs that inhibited 90% of growth (MIC_{90}) were determined from the visual presence or absence of growth in biological triplicates. The fractional inhibitory concentration index (FICI) was determined for RNase HI inhibitors in combination with rifampicin by the addition of a sub-MIC of rifampicin (5 nM) to the MIC assay. FICI values were calculated using the equation $FICI = FIC_A + FIC_B = (C_A/MIC_A) + (C_B/MIC_B)$, where MIC_A and MIC_B are the MICs of drugs A and B alone, and C_A and C_B are the concentrations of the drugs in combination.

Recombinant RnhC purification. The open reading frame (ORF) encoding RnhC (Rv2228c) was amplified from *M. tuberculosis* genomic DNA and cloned into pMAL-C2 (95) to produce an N-terminal maltose-binding protein (MBP) fusion construct which was modified to include a His$_6$ tag and a 3C protease recognition sequence (96) immediately upstream of the RnhC sequence. The plasmid was transformed into *E. coli* BL21(DE3)pLysS (97). Protein was produced by auto-induction of cultures grown in ZYP-5052 medium (98) for 7 h at 37°C and then for 20 h at 28°C. The cells were harvested (5,300 $\times$ g for 30 min at 4°C) and resuspended in lysis buffer (20 mM HEPES and 150 mM NaCl, pH 7.5) containing 10 μg/mL of DNase I and one cOmplete Mini EDTA-free protease inhibitor tablet (Roche) per 10 mL total volume. The cells were lysed using a cell disruptor (Constant Systems) at a pressure of 18 kilopounds per square inch (kpsi). The lysate was centrifuged at 20,000 $\times$ g for 30 min at 4°C. Recombinant RnhC was purified by affinity chromatography using an amylose column and cleaved from the tags (MBP and His$_6$) by overnight incubation of His$_6$-tagged recombinant 3C protease at 4°C. The 3C protease and the tags were removed by reverse affinity chromatography. RnhC was concentrated and further purified by size exclusion chromatography using a 16/600 Superdex 200 pg column (GE Healthcare). RnhC was eluted in a single peak, concentrated to 10 mg/mL, and stored at -20°C.

HIV-RNase HI inhibitors. Inhibitors of HIV RNase H were selected from the PubChem database and kindly provided by the National Institutes of Health (NIH) through the Developmental Therapeutics Program (DTP). The compounds were resuspended in dimethyl sulfoxide (DMSO) at a final concentration of 10 mM and stored at -20°C.

RNase HI inhibition assay. The RNase HI activity assay was performed using a Förster resonance energy transfer (FRET) assay as previously described (99) using an 18-bp RNA/DNA substrate, with the RNA strand labeled with fluorescein at the 3'-end (5'-GAU-CUG-AGC-CUG-GGA-GCU-fluorescein-3'), and the cDNA strand labeled with Iowa black on the 5'-end (5'-Iowa black-AGC-TCC-CAG-GCT-CAG-ATC-3'). RnhC (4 nM) was incubated with 25 nM substrate in FRET buffer (50 mM Tris-HCl, pH 8, 60 mM KCl, 5 mM $MgCl_2$). The increase in fluorescein signal due to substrate hydrolysis was monitored at excitation/emission wavelengths of 490 nm/528 nm using a SpectraMax iD3 plate reader. Compounds active at an initial concentration of 100 μM were subsequently assessed using a dose-response assay.

SUPPLEMENTAL MATERIAL

Supplemental material is available online only.

SUPPLEMENTAL FILE 1, PDF file, 0.2 MB.

ACKNOWLEDGMENTS

REFERENCES

1. O'Neill J. 2016. Tackling drug-resistant infections globally: final report and recommendations. Wellcome Trust, London, UK.
2. World Health Organisation. 2020. Consolidated guidelines on tuberculosis. https://www.who.int/publications/i/item/9789240007048.
3. Conradie F, Diacon AH, Ngubane N, Howell P, Everitt D, Crook AM, Mendel CM, Egizi E, Moreira J, Timm J, McHugh TD, Wills GH, Bateson A, Hunt R, Van Niekerk C, Li M, Olugbosi M, Spigelman M, Nix TBTT, Nix-TB Trial Team. 2020. Treatment of highly drug-resistant pulmonary tuberculosis. N Engl J Med 382:893–902. https://doi.org/10.1056/NEJMoa1901814.
4. Thomas M, White RL, Davis RW. 1976. Hybridization of RNA to double-stranded DNA: formation of R-loops. Proc Natl Acad Sci U S A 73:2294–2298. https://doi.org/10.1073/pnas.73.7.2294.
5. Drolet M, Phoenix P, Menzel R, Massé E, Liu LF, Crouch RJ. 1995. Overexpression of RNase H partially complements the growth defect of an *Escherichia coli* Δ*topA* mutant: R-loop formation is a major problem in the absence of DNA topoisomerase I. Proc Natl Acad Sci U S A 92:3526–3530. https://doi.org/10.1073/pnas.92.8.3526.
6. Alzu A, Bermejo R, Begnis M, Lucca C, Piccini D, Carotenuto W, Saponaro M, Brambati A, Cocito A, Foiani M, Liberi G. 2012. Senataxin associates with replication forks to protect fork integrity across RNA-polymerase-II-transcribed genes. Cell 151:835–846. https://doi.org/10.1016/j.cell.2012.09.041.
7. Santos-Pereira JM, Herrero AB, Garcia-Rubio ML, Marin A, Moreno S, Aguilera A. 2013. The Npl3 hnRNP prevents R-loop-mediated transcription-replication conflicts and genome instability. Genes Dev 27:2445–2458. https://doi.org/10.1101/gad.229880.113.
8. Dominguez-Sanchez MS, Barroso S, Gomez-Gonzalez B, Luna R, Aguilera A. 2011. Genome instability and transcription elongation impairment in human cells depleted of THO/TREX. PLoS Genet 7:e1002386. https://doi.org/10.1371/journal.pgen.1002386.
9. Tuduri S, Crabbe L, Conti C, Tourriere H, Holtgreve-Grez H, Jauch A, Pantesco V, De Vos J, Thomas A, Theillet C, Pommier Y, Tazi J, Coquelle A, Pasero P. 2009. Topoisomerase I suppresses genomic instability by preventing interference between replication and transcription. Nat Cell Biol 11:1315–1324. https://doi.org/10.1038/ncb1984.
10. Dasgupta S, Masukata H, Tomizawa J. 1987. Multiple mechanisms for initiation of ColE1 DNA replication: DNA synthesis in the presence and absence of ribonuclease H. Cell 51:1113–1122. https://doi.org/10.1016/0092-8674(87)90597-6.
11. Ivančić-Baće I, Al Howard J, Bolt EL. 2012. Tuning in to interference: R-loops and cascade complexes in CRISPR immunity. J Mol Biol 422:607–616. https://doi.org/10.1016/j.jmb.2012.06.024.
12. Stein H, Hausen P. 1969. Enzyme from calf thymus degrading the RNA moiety of DNA-RNA Hybrids: effect on DNA-dependent RNA polymerase. Science 166:393–395. https://doi.org/10.1126/science.166.3903.393.
13. Balbontín R, Frazão N, Gordo I. 2021. DNA breaks-mediated fitness cost reveals RNase HI as a new target for selectively eliminating antibiotic-resistant bacteria. Mol Biol Evol 38:3220–3234. https://doi.org/10.1093/molbev/msab093.
14. Ilina TV, Brosenitsch T, Sluis-Cremer N, Ishima R. 2021. Retroviral RNase H: structure, mechanism, and inhibition, p 227–247. *In* Cameron CE, Arnold JJ, Kaguni LS (ed), The enzymes, vol 50. Academic Press, San Diego, CA.
15. Kankanala J, Kirby KA, Huber AD, Casey MC, Wilson DJ, Sarafianos SG, Wang Z. 2017. Design, synthesis and biological evaluations of N-hydroxy thienopyrimidine-2,4-diones as inhibitors of HIV reverse transcriptase-associated RNase H. Eur J Med Chem 141:149–161. https://doi.org/10.1016/j.ejmech.2017.09.054.
16. Vernekar SKV, Tang J, Wu B, Huber AD, Casey MC, Myshakina N, Wilson DJ, Kankanala J, Kirby KA, Parniak MA, Sarafianos SG, Wang Z. 2017. Double-winged 3-hydroxypyrimidine-2,4-diones: potent and selective inhibition against HIV-1 RNase H with significant antiviral activity. J Med Chem 60:5045–5056. https://doi.org/10.1021/acs.jmedchem.7b00440.
17. Watkins HA, Baker EN. 2010. Structural and functional characterization of an RNase HI domain from the bifunctional protein Rv2228c from *Mycobacterium tuberculosis*. J Bacteriol 192:2878–2886. https://doi.org/10.1128/JB.01615-09.
18. Minias AE, Brzostek AM, Korycka- Machala M, Dziadek B, Minias P, Rajagopalan M, Madiraju M, Dziadek J. 2015. RNase HI is essential for survival of *Mycobacterium smegmatis*. PLoS One 10:e0126260. https://doi.org/10.1371/journal.pone.0126260.
19. Gupta R, Chatterjee D, Glickman MS, Shuman S. 2017. Division of labor among *Mycobacterium smegmatis* RNase H enzymes: RNase HI activity of RnhA or RnhC is essential for growth whereas RnhB and RnhA guard against killing by hydrogen peroxide in stationary phase. Nucleic Acids Res 45:1–14. https://doi.org/10.1093/nar/gkw1046.
20. Czubat B, Minias A, Brzostek A, Żaczek A, Struś K, Zakrzewska-Czerwińska J, Dziadek J. 2020. Functional disassociation between the protein domains of MSMEG_4305 of *Mycolicibacterium smegmatis* (*Mycobacterium smegmatis*) *in vivo*. Front Microbiol 11:1–14. https://doi.org/10.3389/fmicb.2020.02008.
21. Jacewicz A, Shuman S. 2015. Biochemical characterization of *Mycobacterium smegmatis* RnhC (MSMEG_4305), a bifunctional enzyme composed of autonomous N-terminal type I RNase H and C-terminal acid phosphatase domains. J Bacteriol 197:2489–2498. https://doi.org/10.1128/JB.00268-15.
22. Lamichhane G, Zignol M, Blades NJ, Geiman DE, Dougherty A, Grosset J, Broman KW, Bishai WR. 2003. A postgenomic method for predicting essential genes at subsaturation levels of mutagenesis: application to *Mycobacterium tuberculosis*. Proc Natl Acad Sci U S A 100:7213–7218. https://doi.org/10.1073/pnas.1231432100.
23. Griffin JE, Gawronski JD, Dejesus MA, Ioerger TR, Akerley BJ, Sassetti CM. 2011. High-resolution phenotypic profiling defines genes essential for mycobacterial growth and cholesterol catabolism. PLoS Pathog 7:e1002251. https://doi.org/10.1371/journal.ppat.1002251.
24. Boguslawski SJ, Smith DE, Michalak MA, Mickelson KE, Yehle CO, Patterson WL, Carrico RJ. 1986. Characterization of monoclonal antibody to DNA.RNA and its application to immunodetection of hybrids. J Immunol Methods 89:123–130. https://doi.org/10.1016/0022-1759(86)90040-2.
25. Hong X, Cadwell GW, Kogoma T. 1995. *Escherichia coli* RecG and RecA proteins in R-loop formation. EMBO J 14:2385–2392. https://doi.org/10.1002/j.1460-2075.1995.tb07233.x.
26. Stolz R, Sulthana S, Hartono SR, Malig M, Benham CJ, Chedin F. 2019. Interplay between DNA sequence and negative superhelicity drives R-loop structures. Proc Natl Acad Sci U S A 116:6260–6269. https://doi.org/10.1073/pnas.1819476116.
27. Belotserkovskii BP, Soo Shin JH, Hanawalt PC. 2017. Strong transcription blockage mediated by R-loop formation within a G-rich homopurine-homopyrimidine sequence localized in the vicinity of the promoter. Nucleic Acids Res 45:6589–6599. https://doi.org/10.1093/nar/gkx403.
28. Tous C, Aguilera A. 2007. Impairment of transcription elongation by R-loops in vitro. Biochem Biophys Res Commun 360:428–432. https://doi.org/10.1016/j.bbrc.2007.06.098.
29. Deng S, Stein RA, Higgins NP. 2004. Transcription-induced barriers to supercoil diffusion in the *Salmonella typhimurium* chromosome. Proc Natl Acad Sci U S A 101:3398–3403. https://doi.org/10.1073/pnas.0307550101.
30. Ahmed W, Sala C, Hegde SR, Jha RK, Cole ST, Nagaraja V. 2017. Transcription facilitated genome-wide recruitment of topoisomerase I and DNA gyrase. PLoS Genet 13:e1006754. https://doi.org/10.1371/journal.pgen.1006754.
31. Unniraman S, Nagaraja V. 1999. Regulation of DNA gyrase operon in *Mycobacterium smegmatis*: a distinct mechanism of relaxation stimulated transcription. Genes Cells 4:697–706. https://doi.org/10.1046/j.1365-2443.1999.00296.x.
32. Ahmed W, Menon S, D NB, Karthik PV, Nagaraja V. 2016. Autoregulation of topoisomerase I expression by supercoiling sensitive transcription. Nucleic Acids Res 44:1541–1552. https://doi.org/10.1093/nar/gkv1088.

33. Kogoma T. 1984. Absence of RNase H allows replication of pBR322 in *Escherichia coli* mutants lacking DNA polymerase I. Proc Natl Acad Sci U S A 81:7845–7849. https://doi.org/10.1073/pnas.81.24.7845.

34. Harinarayanan R, Gowrishankar J. 2003. Host factor titration by chromosomal R-loops as a mechanism for runaway plasmid replication in transcription termination-defective mutants of *Escherichia coli*. J Mol Biol 332: 31–46. https://doi.org/10.1016/s0022-2836(03)00753-8.

35. Biek DP, Cohen SN. 1989. Involvement of integration host factor (IHF) in maintenance of plasmid pSC101 in *Escherichia coli*: mutations in the *topA* gene allow pSC101 replication in the absence of IHF. J Bacteriol 171: 2066–2074. https://doi.org/10.1128/jb.171.4.2066-2074.1989.

36. Chatterjee S, Basu A, Basu A, Das Gupta SK. 2007. DNA bending in the mycobacterial plasmid pAL5000 origin-RepB complex. J Bacteriol 189: 8584–8592. https://doi.org/10.1128/JB.01155-07.

37. Maduike NZ, Tehranchi AK, Wang JD, Kreuzer KN. 2014. Replication of the *Escherichia coli* chromosome in RNase HI-deficient cells: multiple initiation regions and fork dynamics. Mol Microbiol 91:39–56. https://doi.org/10.1111/mmi.12440.

38. Ranes MG, Rauzier J, Lagranderie M, Gheorghiu M, Gicquel B. 1990. Functional analysis of pAL5000, a plasmid from *Mycobacterium fortuitum*: construction of a "mini" mycobacterium-*Escherichia coli* shuttle vector. J Bacteriol 172:2793–2797. https://doi.org/10.1128/jb.172.5.2793-2797.1990.

39. Chatterjee S, Patra MM, Samaddar S, Basu A, Das Gupta SK. 2017. Mutual interaction enables the mycobacterial plasmid pAL5000 origin binding protein RepB to recruit RepA, the plasmid replicase, to the origin. Microbiology (Reading) 163:595–610. https://doi.org/10.1099/mic.0.000447.

40. Bourn WR, Jansen Y, Stutz H, Warren RM, Williamson AL, van Helden PD. 2007. Creation and characterisation of a high-copy-number version of the pAL5000 mycobacterial replicon. Tuberculosis (Edinb) 87:481–488. https://doi.org/10.1016/j.tube.2007.08.003.

41. McClure WR, Cech CL. 1978. On the mechanism of rifampicin inhibition of RNA synthesis. J Biol Chem 253:8949–8956. https://doi.org/10.1016/S0021-9258(17)34269-2.

42. Drlica K, Franco RJ, Steck TR. 1988. Rifampin and rpoB mutations can alter DNA supercoiling in *Escherichia coli*. J Bacteriol 170:4983–4985. https://doi.org/10.1128/jb.170.10.4983-4985.1988.

43. Broccoli S, Rallu F, Sanscartier P, Cerritelli SM, Crouch RJ, Drolet M. 2004. Effects of RNA polymerase modifications on transcription-induced negative supercoiling and associated R-loop formation. Mol Microbiol 52: 1769–1779. https://doi.org/10.1111/j.1365-2958.2004.04092.x.

44. Mangiameli SM, Veit BT, Merrikh H, Wiggins PA. 2017. The replisomes remain spatially proximal throughout the cell cycle in bacteria. PLoS Genet 13:e1006582. https://doi.org/10.1371/journal.pgen.1006582.

45. Agrawal P, Miryala S, Varshney U. 2015. Use of *Mycobacterium smegmatis* deficient in ADP-ribosyltransferase as surrogate for *Mycobacterium tuberculosis* in drug testing and mutation analysis. PLoS One 10:e0122076. https://doi.org/10.1371/journal.pone.0122076.

46. Li X-Z, Zhang L, Nikaido H. 2004. Efflux pump-mediated intrinsic drug resistance in *Mycobacterium smegmatis*. Antimicrob Agents Chemother 48: 2415–2423. https://doi.org/10.1128/AAC.48.7.2415-2423.2004.

47. Gowrishankar J, Harinarayanan R. 2004. Why is transcription coupled to translation in bacteria? Mol Microbiol 54:598–603. https://doi.org/10.1111/j.1365-2958.2004.04289.x.

48. Massé E, Drolet M. 1999. R-loop-dependent hypernegative supercoiling in *Escherichia coli* topA mutants preferentially occurs at low temperatures and correlates with growth inhibition. J Mol Biol 294:321–332. https://doi.org/10.1006/jmbi.1999.3264.

49. Yang Z, Hou Q, Cheng L, Xu W, Hong Y, Li S, Sun Q. 2017. RNase H1 cooperates with DNA gyrases to restrict R-loops and maintain genome integrity in *Arabidopsis* chloroplasts. Plant Cell 29:2478–2497. https://doi.org/10.1105/tpc.17.00305.

50. Winder FG, Collins PB. 1970. Inhibition by isoniazid of synthesis of mycolic acids in *Mycobacterium tuberculosis*. J Gen Microbiol 63:41–48. https://doi.org/10.1099/00221287-63-1-41.

51. Chen J, Raymond K. 2006. Roles of rifampicin in drug-drug interactions: underlying molecular mechanisms involving the nuclear pregnane X receptor. Ann Clin Microbiol Antimicrob 5:3. https://doi.org/10.1186/1476-0711-5-3.

52. Boyer PL, Smith SJ, Zhao XZ, Das K, Gruber K, Arnold E, Burke TR, Hughes SH. 2018. Developing and Evaluating Inhibitors against the RNase H Active Site of HIV-1 Reverse Transcriptase. J Virol 92:e02203-17. https://doi.org/10.1128/JVI.02203-17.

53. Poongavanam V, Corona A, Steinmann C, Scipione L, Grandi N, Pandolfi F, Di Santo R, Costi R, Esposito F, Tramontano E, Kongsted J. 2018. Structure-guided

approach identifies a novel class of HIV-1 ribonuclease H inhibitors: binding mode insights through magnesium complexation and site-directed mutagenesis studies. Med Chem Commun (Camb) 9:562–575. https://doi.org/10.1039/C7MD00600D.

54. Cao L, Song W, De Clercq E, Zhan P, Liu X. 2014. Recent progress in the research of small molecule HIV-1 RNase H inhibitors. Curr Med Chem 21: 1956–1967. https://doi.org/10.2174/0929867321666140120121158.

55. Lang KS, Hall AN, Merrikh CN, Ragheb M, Tabakh H, Pollock AJ, Woodward JJ, Dreifus JE, Merrikh H. 2017. Replication-transcription conflicts generate R-loops that orchestrate bacterial stress survival and pathogenesis. Cell 170:787–799.e18. https://doi.org/10.1016/j.cell.2017.07.044.

56. Wahba L, Amon JD, Koshland D, Vuica-Ross M. 2011. RNase H and multiple RNA biogenesis factors cooperate to prevent RNA:DNA hybrids from generating genome instability. Mol Cell 44:978–988. https://doi.org/10.1016/j.molcel.2011.10.017.

57. Amon JD, Koshland D. 2016. RNase H enables efficient repair of R-loop induced DNA damage. Elife 5:e20533. https://doi.org/10.7554/eLife.20533.

58. Parajuli S, Teasley DC, Murali B, Jackson J, Vindigni A, Stewart SA. 2017. Human ribonuclease H1 resolves R-loops and thereby enables progression of the DNA replication fork. J Biol Chem 292:15216–15224. https://doi.org/10.1074/jbc.M117.787473.

59. Dutta D, Shatalin K, Epshtein V, Gottesman ME, Nudler E. 2011. Linking RNA polymerase backtracking to genome instability in *E. coli*. Cell 146: 533–543. https://doi.org/10.1016/j.cell.2011.07.034.

60. Zatreanu D, Han Z, Mitter R, Tumini E, Williams H, Gregersen L, Dirac-Svejstrup AB, Roma S, Stewart A, Aguilera A, Svejstrup JQ. 2019. Elongation factor TFIIS prevents transcription stress and R-loop accumulation to maintain genome stability. Mol Cell 76:57–69.e9. https://doi.org/10.1016/j.molcel.2019.07.037.

61. Zhang X, Chiang HC, Wang Y, Zhang C, Smith S, Zhao X, Nair SJ, Michalek J, Jatoi I, Lautner M, Oliver B, Wang H, Petit A, Soler T, Brunet J, Mateo F, Angel Pujana M, Poggi E, Chaldekas K, Isaacs C, Peshkin BN, Ochoa O, Chedin F, Theoharis C, Sun LZ, Curiel TJ, Elledge R, Jin VX, Hu Y, Li R. 2017. Attenuation of RNA polymerase II pausing mitigates BRCA1-associated R-loop accumulation and tumorigenesis. Nat Commun 8:15908. https://doi.org/10.1038/ncomms15908.

62. Wu HY, Shyy SH, Wang JC, Liu LF. 1988. Transcription generates positively and negatively supercoiled domains in the template. Cell 53:433–440. https://doi.org/10.1016/0092-8674(88)90163-8.

63. Tsao Y-P, Wu H-Y, Liu LF. 1989. Transcription-driven supercoiling of DNA: Direct biochemical evidence from *in vitro* studies. Cell 56:111–118. https://doi.org/10.1016/0092-8674(89)90989-6.

64. Tantale K, Mueller F, Kozulic-Pirher A, Lesne A, Victor J-M, Robert M-C, Capozi S, Chouaib R, Bäcker V, Mateos-Langerak J, Darzacq X, Zimmer C, Basyuk E, Bertrand E. 2016. A single-molecule view of transcription reveals convoys of RNA polymerases and multi-scale bursting. Nat Commun 7: 12248. https://doi.org/10.1038/ncomms12248.

65. Lesne A, Victor JM, Bertrand E, Basyuk E, Barbi M. 2018. The role of supercoiling in the motor activity of RNA polymerases. Methods Mol Biol 1805: 215–232. https://doi.org/10.1007/978-1-4939-8556-2_11.

66. Fujita K, Iwaki M, Yanagida T. 2016. Transcriptional bursting is intrinsically caused by interplay between RNA polymerases on DNA. Nat Commun 7: 13788. https://doi.org/10.1038/ncomms13788.

67. Jin J, Bai L, Johnson DS, Fulbright RM, Kireeva ML, Kashlev M, Wang MD. 2010. Synergistic action of RNA polymerases in overcoming the nucleosomal barrier. Nat Struct Mol Biol 17:745–752. https://doi.org/10.1038/nsmb.1798.

68. Golding I, Paulsson J, Zawilski SM, Cox EC. 2005. Real-time kinetics of gene activity in individual bacteria. Cell 123:1025–1036. https://doi.org/10.1016/j.cell.2005.09.031.

69. So LH, Ghosh A, Zong C, Sepúlveda LA, Segev R, Golding I. 2011. General properties of transcriptional time series in *Escherichia coli*. Nat Genet 43: 554–560. https://doi.org/10.1038/ng.821.

70. Engl C, Jovanovic G, Brackston RD, Kotta-Loizou I, Buck M. 2020. The route to transcription initiation determines the mode of transcriptional bursting in *E. coli*. Nat Commun 11:2422. https://doi.org/10.1038/s41467-020-16367-6.

71. Epshtein V, Nudler E. 2003. Cooperation between RNA polymerase molecules in transcription elongation. Science 300:801–805. https://doi.org/10.1126/science.1083219.

72. Figueroa N, Bossi L. 1988. Transcription induces gyration of the DNA template in *Escherichia coli*. Proc Natl Acad Sci U S A 85:9416–9420. https://doi.org/10.1073/pnas.85.24.9416.

73. Hu Y, Mangan JA, Dhillon J, Sole KM, Mitchison DA, Butcher PD, Coates AR. 2000. Detection of mRNA transcripts and active transcription in persistent *Mycobacterium tuberculosis* induced by exposure to rifampin or pyrazinamide. J Bacteriol 182:6358–6365. https://doi.org/10.1128/JB.182 .22.6358-6365.2000.

74. Stevenson-Jones F, Woodgate J, Castro-Roa D, Zenkin N. 2020. Ribosome reactivates transcription by physically pushing RNA polymerase out of transcription arrest. Proc Natl Acad Sci U S A 117:8462–8467. https://doi .org/10.1073/pnas.1919985117.

75. Cokol M, Kuru N, Bicak E, Larkins-Ford J, Aldridge BB. 2017. Efficient measurement and factorization of high-order drug interactions in *Mycobacterium tuberculosis*. Sci Adv 3:e1701881. https://doi.org/10.1126/sciadv .1701881.

76. Malik M, Zhao X, Drlica K. 2006. Lethal fragmentation of bacterial chromosomes mediated by DNA gyrase and quinolones. Mol Microbiol 61: 810–825. https://doi.org/10.1111/j.1365-2958.2006.05275.x.

77. Godbole AA, Ahmed W, Bhat RS, Bradley EK, Ekins S, Nagaraja V. 2014. Inhibition of *Mycobacterium tuberculosis* topoisomerase I by m-AMSA, a eukaryotic type II topoisomerase poison. Biochem Biophys Res Commun 446:916–920. https://doi.org/10.1016/j.bbrc.2014.03.029.

78. Rawal P, Kummarasetti VB, Ravindran J, Kumar N, Halder K, Sharma R, Mukerji M, Das SK, Chowdhury S. 2006. Genome-wide prediction of G4 DNA as regulatory motifs: role in *Escherichia coli* global regulation. Genome Res 16:644–655. https://doi.org/10.1101/gr.4508806.

79. Gomez-Gonzalez B, Garcia-Rubio M, Bermejo R, Gaillard H, Shirahige K, Marin A, Foiani M, Aguilera A. 2011. Genome-wide function of THO/TREX in active genes prevents R-loop-dependent replication obstacles. EMBO J 30:3106–3119. https://doi.org/10.1038/emboj.2011.206.

80. Gan W, Guan Z, Liu J, Gui T, Shen K, Manley JL, Li X. 2011. R-loop-mediated genomic instability is caused by impairment of replication fork progression. Genes Dev 25:2041–2056. https://doi.org/10.1101/gad.17010011.

81. O'Connell K, Jinks-Robertson S, Petes TD. 2015. Elevated genome-wide instability in yeast mutants lacking RNase H activity. Genetics 201:963–975. https://doi.org/10.1534/genetics.115.182725.

82. Li X, Manley JL. 2005. Inactivation of the SR protein splicing factor ASF/ SF2 results in genomic instability. Cell 122:365–378. https://doi.org/10 .1016/j.cell.2005.06.008.

83. Hatchi E, Skourti-Stathaki K, Ventz S, Pinello L, Yen A, Kamieniarz-Gdula K, Dimitrov S, Pathania S, McKinney KM, Eaton ML, Kellis M, Hill SJ, Parmigiani G, Proudfoot NJ, Livingston DM. 2015. BRCA1 recruitment to transcriptional pause sites is required for R-loop-driven DNA damage repair. Mol Cell 57:636–647. https://doi.org/10.1016/j.molcel.2015.01.011.

84. Sordet O, Redon CE, Guirouilh-Barbat J, Smith S, Solier S, Douarre C, Conti C, Nakamura AJ, Das BB, Nicolas E, Kohn KW, Bonner WM, Pommier Y. 2009. Ataxia telangiectasia mutated activation by transcription- and topoisomerase I-induced DNA double-strand breaks. EMBO Rep 10:887–893. https:// doi.org/10.1038/embor.2009.97.

85. Parish T, Stoker NG. 2000. Use of a flexible cassette method to generate a double unmarked *Mycobacterium tuberculosis tlyA plcABC* mutant by gene replacement. Microbiology 146:1969–1975. https://doi.org/10.1099/ 00221287-146-8-1969.

86. Andreu N, Zelmer A, Fletcher T, Elkington PT, Ward TH, Ripoll J, Parish T, Bancroft GJ, Schaible U, Robertson BD, Wiles S. 2010. Optimisation of bioluminescent reporters for use with mycobacteria. PLoS One 5:e10777. https://doi.org/10.1371/journal.pone.0010777.

87. Rauzier J, Moniz-Pereira J, Gicquel-Sanzey B. 1988. Complete nucleotide sequence of pAL5OOO, a plasmid from *Mycobacterium fortuitum*. Gene 71:315–321. https://doi.org/10.1016/0378-1119(88)90048-0.

88. Machowski EE, Dawes S, Mizrahi V. 2005. TB tools to tell the tale-molecular genetic methods for mycobacterial research. Int J Biochem Cell Biol 37:54–68. https://doi.org/10.1016/j.biocel.2004.06.012.

89. Dawes SS, Crouch RJ, Morris SL, Mizrahi V. 1995. Cloning, sequence analysis, overproduction in *Escherichia coli* and enzymatic characterization of the RNase HI from *Mycobacterium smegmatis*. Gene 165:71–75. https:// doi.org/10.1016/0378-1119(95)00523-9.

90. Downing KJ, McAdam RA, Mizrahi V. 1999. *Staphylococcus aureus* nuclease is a useful secretion reporter for mycobacteria. Gene 239:293–299. https://doi.org/10.1016/s0378-1119(99)00408-4.

91. Belisle JT, Mahaffey SB, Hill PJ. 2009. Isolation of mycobacterium species genomic DNA. Methods Mol Biol 465:1–12. https://doi.org/10.1007/978-1 -59745-207-6_1.

92. Miller J. 1972. Assay of β-galactosidase in: experiments in molecular genetics. Cold Spring Harbor Laboratory Press, Cold Spring Harbor, New York.

93. Griffith KL, Wolf RE, Jr. 2002. Measuring β-galactosidase activity in bacteria: cell growth, permeabilization, and enzyme assays in 96-well arrays. Biochem Biophys Res Commun 290:397–402. https://doi.org/10.1006/ bbrc.2001.6152.

94. Sambandamurthy VK, Derrick SC, Hsu T, Chen B, Larsen MH, Jalapathy KV, Chen M, Kim J, Porcelli SA, Chan J, Morris SL, Jacobs WR, Jr. 2006. *Mycobacterium tuberculosis* ΔRD1 Δ*panCD*: a safe and limited replicating mutant strain that protects immunocompetent and immunocompromised mice against experimental tuberculosis. Vaccine 24:6309–6320. https://doi.org/ 10.1016/j.vaccine.2006.05.097.

95. Walker IH, Hsieh PC, Riggs PD. 2010. Mutations in maltose-binding protein that alter affinity and solubility properties. Appl Microbiol Biotechnol 88:187–197. https://doi.org/10.1007/s00253-010-2696-y.

96. Cordingley MG, Callahan PL, Sardana VV, Garsky VM, Colonno RJ. 1990. Substrate requirements of human rhinovirus 3C protease for peptide cleavage *in vitro*. J Biol Chem 265:9062–9065. https://doi.org/10.1016/ S0021-9258(19)38811-8.

97. Studier FW, Moffatt BA. 1986. Use of bacteriophage T7 RNA polymerase to direct selective high-level expression of cloned genes. J Mol Biol 189: 113–130. https://doi.org/10.1016/0022-2836(86)90385-2.

98. Studier FW. 2005. Protein production by auto-induction in high density shaking cultures. Protein Expr Purif 41:207–234. https://doi.org/10.1016/j .pep.2005.01.016.

99. Parniak MA, Min K-L, Budihas SR, Le Grice SFJ, Beutler JA. 2003. A fluorescence-based high-throughput screening assay for inhibitors of human immunodeficiency virus-1 reverse transcriptase-associated ribonuclease H activity. Anal Biochem 322:33–39. https://doi.org/10.1016/j.ab.2003.06 .001.